Novel analogues of the therapeutic complement inhibitor compstatin with significantly improved affinity and potency

Hongchang Qu [a,1], Paola Magotti [a,1], Daniel Ricklin [a], Emilia L. Wu [b], Ioannis Kourtzelis [a], You-Qiang Wu [a], Yiannis N. Kaznessis [b], John D. Lambris [a,*]

[a] Department of Pathology and Laboratory Medicine, University of Pennsylvania, Philadelphia, PA 19104, USA
[b] Department of Chemical Engineering and Materials Science, University of Minnesota, Minneapolis, MN 55455, USA

ARTICLE INFO

ABSTRACT

Compstatin is a 13-residue disulfide-bridged peptide that inhibits a key step in the activation of the human complement system. Compstatin and its derivatives have shown great promise for the treatment of many clinical disorders associated with unbalanced complement activity. To obtain more potent compstatin analogues, we have now performed an N-methylation scan of the peptide backbone and amino acid substitutions at position 13. One analogue (Ac-I[CVW(Me)QDW-Sar-AHRC](NMe)I-NH$_2$) displayed a 1000-fold increase in both potency (IC$_{50}$ = 62 nM) and binding affinity for C3b (K_D = 2.3 nM) over that of the original compstatin. Biophysical analysis using surface plasmon resonance and isothermal titration calorimetry suggests that the improved binding originates from more favorable free conformation and stronger hydrophobic interactions. This study provides a series of significantly improved drug leads for therapeutic applications in complement-related diseases, and offers new insights into the structure–activity relationships of compstatin analogues.

1. Introduction

The human complement system is an integral part of innate immunity that acts as a surveillance and clearance system of the human body (Mastellos et al., 2004; Ricklin et al., 2010). When complement recognizes foreign surfaces, its intricate network of membrane-bound and fluid-phase proteins is activated through several initiation pathways, which all result in the generation of strong opsonins, the lytic membrane attack complex, and pro-inflammatory anaphylatoxins. These processes are essential to the elimination of invading microorganisms, the clearance of immune complexes and apoptotic cells, and the stimulation of adaptive immune responses (Carroll, 2008; Sjoberg et al., 2009). However, inappropriate or uncontrolled activation of complement can cause damage to host cells or serious disturbance of homeostasis, and it has been associated with a wide array of autoimmune, inflammatory, and neurodegenerative disorders, including rheumatoid arthritis, systemic lupus erythematosus, age-related macular degeneration, sepsis, and Alzheimer's disease (Chen et al., 2010; Lachmann and Smith, 2009; Mollnes and Kirschfink, 2006). Excessive activation of complement has also been linked to ischemia-reperfusion injuries, as seen in stroke or during cardiopulmonary bypass surgery (Diepenhorst et al., 2009; Weisman et al., 1990). In addition, complement has recently been shown to contribute to tumor growth in mice (Markiewski et al., 2008).

Therapeutic inhibition of complement has been found to be highly beneficial in numerous disease studies involving both low molecular weight and biopharmaceutical complement inhibitors (Qu et al., 2009b; Ricklin and Lambris, 2007). The U.S. Food and Drug Administration has approved two complement-targeting drugs thus far, recombinant C1 esterase inhibitor (Cinryze, ViroPharma; Berinert, CSL Behring) for treating hereditary angioedema and the therapeutic antibody Eculizumab (Soliris, Alexion Pharmaceuticals) for paroxysmal nocturnal hemoglobinuria (Cocchio and Marzella, 2009; Inoue et al., 2003; Rother et al., 2007). In addition, a host of complement inhibitors are currently in clinical trials or in advanced pre-clinical development for various indications (Qu et al., 2009b; Ricklin and Lambris, 2007).

Owing to their excellent safety and efficacy profiles and their ability to block activation of complement regardless of the initiation pathway, compstatin derivatives are considered among the most

---

promising of candidate drugs for preventing undesirable effects of complement (Ricklin and Lambris, 2008). One compstatin analogue (POT-4; Potentia Pharmaceuticals & Alcon Inc.) has demonstrated beneficial results in a recently completed Phase I clinical trial for the treatment of age-related macular degeneration and is likely to be further developed for both wet and dry forms of the disease (Anon., 2009). In addition, compstatin has shown highly promising effects in a number of other diseases, as very recently in the case of sepsis (Silasi-Mansat et al., 2010) and complement-related adverse effects during hemodialysis (Kourtzelis et al., 2010). Finally, compstatin is widely used as a valuable tool in immunological research for investigating the effect of the complement cascade in both physiological and pathophysiological processes.

Compstatin was originally identified as a 13-residue disulfide-bridged peptide (H-Ile-[Cys-Val-Val-Gln-Asp-Trp-Gly-His-His-Arg-Cys]-Thr-NH$_2$) that selectively binds to human and primate forms of the central complement component C3 and its active fragment, C3b (Sahu et al., 1996). It thereby prevents the essential conversion of C3 to C3b and simultaneously impairs all initiation, amplification, and terminal pathways of complement. Over the past decade, extensive structure–activity relationship studies of compstatin have been conducted with the aid of computational molecular modeling and biophysical analysis (Klepeis et al., 2003; Magotti et al., 2009; Ricklin and Lambris, 2007, 2008; Soulika et al., 2003). This work has led to the development of [Trp(Me)^4]-Ac-compstatin (Ac-Ile-[Cys-Val-Trp(Me)-Gln-Asp-Trp-Gly-Ala-His-Arg-Cys]-Thr-NH$_2$), which displays the highest inhibitory activity reported thus far: a 264-fold increase in potency (IC$_{50}$ = 205 nM) over the original compstatin in inhibiting complement activation (Katragadda et al., 2006).

Despite these impressive improvements, the development of more potent and stable compstatin analogues is still desirable, given the high plasma concentration of C3 (0.75–1.35 mg/mL) and the limited half-life of compstatin in vivo (Qu et al., 2009a; Soulika et al., 2000). Such analogues would provide greater therapeutic value and allow broader clinical applications. In the present study, we began by analyzing the previously reported data from surface plasmon resonance (SPR) and isothermal titration calorimetry (ITC) assays, which are very useful guides for rational drug development effects (Carbonell and Freire, 2005; Huber, 2005; Sarver et al., 2007; Zhu et al., 2009). We noticed that the binding of compstatin analogues to C3 is predominantly enthalpy-driven and features large entropic penalties, a situation that is in sharp contrast to that observed for compounds such as statins or HIV protease inhibitors, which generally show favorable entropy terms (Freire, 2008). In the case of [Trp(Me)^4]-Ac-compstatin, for example, the highly favorable enthalpy of −17.6 kcal/mol is largely compensated by an unfavorable entropy of 6.9 kcal/mol (Katragadda et al., 2006). These studies clearly indicated that there is still room for further improvement in terms of decreasing entropy.

One of the ways to decrease the binding-related entropy of peptides is backbone N-methylation, which has been shown to provide local constraints to the peptide backbone and thereby affect both secondary structure and side chain orientation (Fairlie et al., 1995; Laufer et al., 2009; Moretto et al., 2006). Such modifications have been shown to offer several potential benefits, including enhanced binding or receptor selectivity, increased half-life in plasma, and improved cell membrane penetration (Chatterjee et al., 2008; Rovero et al., 1989; Weltrowska et al., 2010). Therefore, we performed a mono-N-methylation scan on the [Tyr^4]-Ac-compstatin template (Klepeis et al., 2003). Based on the ELISA results for these analogues, selective N-methylation and amino acid substitutions were then applied to the more potent [Trp(Me)^4]-Ac-compstatin. The most active analogues were further characterized using SPR and ITC. Using this integrated approach, we were able to generate compstatin analogues with significantly improved efficacy and affinity when compared to the previous lead compound.

2. Materials and methods

2.1. Chemicals

Low-loading Rink amide MBHA resin and the following Fmoc-amino acids were obtained from Novabiochem (San Diego, CA): Ile, Cys(Acm), Val, Tyr(tBu), Gln(Trt), Asp(OtBu), Trp(Boc), Gly, Sar, Ala, MeAla, His(Trt), Arg(Pmc), MeIle, Nle, Phe, and Thr(tBu). DIC and Fmoc-Trp(Me)-OH were purchased from AnaSpec (San Jose, CA). HOAt was purchased from Advanced ChemTech (Louisville, KY). NMP and DCM were obtained from Fisher Scientific (Pittsburgh, PA). All other chemical reagents for synthesis were purchased from Sigma–Aldrich (St. Louis, MO) and used without further purification.

2.2. Peptide synthesis and purification

All peptides in this study were synthesized manually by Fmoc solid-phase methodology using DIC and HOAt as coupling reagents. When N-methylated amino acids were not commercially available, N-methylation was performed by using the optimized methodology reported by Biron et al. (2006). The following procedures were used for the synthesis of the linear peptides: Rink amide MBHA resin (294 mg, 0.34 mmol/g) was placed into a 10 mL HSW polypropylene syringe with frits on the bottom (Torviq, Niles, MI) and swollen in DCM (5 mL) for 30 min. After removal of the Fmoc protecting group (25% piperidine in NMP, 5 mL, 5 and 10 min), the resin was washed four times with NMP (5 mL per wash) and DCM (5 mL per wash), and the individual amino acids were coupled to the resin. For each coupling, 3 equivalents (0.3 mmol) of the amino acid, HOAt, and DIC were used, with 10 min preactivation in NMP. All couplings were performed for 1 h and monitored by either the Kaiser test or the chloranil test. In case of a positive test result, the coupling was repeated until a negative test result was observed.

The N-terminal amino group was acetylated with 20 equivalents of acetic anhydride and 2 equivalents of DIPEA in 5 mL of DCM for 30 min. Linear peptides containing Cyc(Acm) residues were cyclized on resin using thallium trifluoroacetate in DMF/anisole (19:1) at ambient temperature for 3 h. The resin was washed four times with DMF, DCM, and DCM/diethylether (1:1) (each 5 mL per wash), and dried under vacuum for 4 h. The peptides were cleaved from the resin with a mixture of 95% TFA, 2.5% water, and 2.5% TIPS for 3 h. After evaporation of the TFA under vacuum, the peptides were precipitated and washed three times with 30 mL of cold diethyl ether per wash. The liquid was separated from the solid by centrifugation and decanted. The crude peptides were dried in air and dissolved in acetonitrile and 0.1% TFA in water (1:3) before purification by preparative RP-HPLC (Vydac C$_{18}$ 218TP152022 column, Western Analytical Products, Murrieta, CA) and elution with a linear gradient of 15–50% acetonitrile in aqueous 0.1% TFA solution over 35 min at a flow rate of 15 mL/min. Fractions containing the desired products were collected, concentrated, and lyophilized. The purified peptides were isolated in 10–15% overall yields and were >95% pure as determined by analytical RP-HPLC (Phenomenex 00G-4041-E0 Luna 5 μm C$_{18}$ 100 Å column, 250 mm × 4.60 mm; Phenomenex, Torrance, CA). The mass of each peptide was confirmed using ThermoQuest Finnigan LCQ Duo and Waters MALDI micro MX instruments.

2.3. Purification of C3

C3 was purified from fresh human plasma obtained from the blood bank of the Hospital of the University of Pennsylvania as described previously (Hammer et al., 1981). In brief, the plasma was

fractionated with 15% (w/v) PEG 3350, and the pellet was resuspended in 20 mM phosphate buffer, pH 7.8, and then subjected to anion-exchange chromatography on a DEAE-HR 40 column (50 cm × 5 cm; Millipore Inc., Billerica, MA) with the same buffer. Proteins were eluted with 6 L of a linear gradient (15–70%) of 20 mM phosphate buffer, pH 7.8, containing 500 mM NaCl. C3 was further purified on a size-exclusion Superdex 200 26/60 column (Amersham Biosciences) and a Mono S column (Amersham Biosciences) to separate C3 from $C3(H_2O)$ (Sahu et al., 2000).

2.4. Inhibition of complement activation

The ability of the compstatin analogues to inhibit complement activation and amplification after initiation by the classical pathway was assessed by ELISA as described elsewhere (Mallik et al., 2005). In brief, complement was activated in human serum using an antigen-antibody complex in the presence or absence of compstatin analogues, and the deposition of C3 fragments on the plate surface was detected using an HRP-conjugated polyclonal anti-C3 antibody. The absorbance data obtained at 405 nm were translated into % inhibition, based on the absorbance corresponding to 100% complement activation in the absence of peptide. The percent inhibition was plotted against the peptide concentration, and the resulting data set was fitted to the logistic dose–response function using Origin 7.0 (OriginLab Corp., Northampton, MA) IC_{50} values were obtained from the fitted parameters that produced the lowest χ^2 value. Each analogue was assayed at least three to seven times using peptides **1** or **14** as internal control. Standard deviations were all within 30% of the mean values.

2.5. ITC analysis

All ITC experiments were performed with the Microcal VP-ITC calorimeter (GE Healthcare Corp., Piscataway, NJ), using protein concentrations of 1.8–5 μM C3 in the cell and peptide concentrations of 40–100 μM of individual compstatin analogues in the syringe. All titrations were performed in PBS (10 mM phosphate buffer with 150 mM NaCl, pH 7.4) at 25 °C using multiple peptide injections of 2–7 μL each. The raw isotherms were corrected for the heats of dilution by subtracting the isotherms representing peptide injections into the buffer. The resulting isotherms were fitted to a single site of sites model using Origin 7.0. The Gibbs free energy was calculated as $\Delta G = \Delta H - T\Delta S$. Each experiment was repeated at least twice. Errors were within 20% of the mean values.

2.6. SPR analysis

The kinetics of the interaction between C3b and each compstatin analogue was analyzed by SPR on a Biacore 3000 instrument (GE Healthcare Corp., Piscataway, NJ) at 25 °C using PBS-T (10 mM sodium phosphate, 150 mM NaCl, 0.005% Tween 20, pH 7.4) as the running buffer, as described previously (Magotti et al., 2009). In brief, biotinylated C3b (30 μg/mL) was immobilized on a streptavidin-coated sensor chip, and a two-fold serial dilution series (1 μM–500 pM) of each analogue was injected for 2 min at 30 μL/min, with a dissociation phase of 5–10 min. Peptide [Trp(Me)^4]-Ac-compstatin was included in each experimental series as an internal control. Data analysis was performed using Scrubber (BioLogic Software, Campbell, Australia). The signals from an untreated flow cell and an ensemble of buffer blank injections were subtracted to correct for buffer effects and injection artifacts. Processed biosensor data were globally fitted to a 1:1 Langmuir binding model, and the equilibrium dissociation constant (K_D) was calculated from the equation $K_D = k_d/k_a$. Peptide solutions were injected in duplicate in every experiment, and each screening assay was performed at least twice. The error of k_a and k_d were within 10% of mean values.

Table 1
Complement inhibition activity of N-methylated analogues of [Tyr^4]-Ac-compstatin (peptide **1**).

Peptide	Sequence	IC_{50} (μM)[a]	IC_{50} fold change[b]
1[c]	Ac-I[CVYQDWGAHRC]T-NH$_2$	2.4	1
2	Ac-I[(NMe)CVYQDWGAHRC]T-NH$_2$	7.5	0.3
3	Ac-I[C(NMe)VYQDWGAHRC]T-NH$_2$	NA	NA
4	Ac-I[CV(NMe)YQDWGAHRC]T-NH$_2$	NA	NA
5	Ac-I[CVY(NMe)QDWGAHRC]T-NH$_2$	33	0.07
6	Ac-I[CVYQ(NMe)DWGAHRC]T-NH$_2$	44	0.06
7	Ac-I[CVYQD(NMe)WGAHRC]T-NH$_2$	25	0.1
8	Ac-I[CVYQDW(NMe)GAHRC]T-NH$_2$	1.4	1.7
9	Ac-I[CVYQDWG(NMe)AHRC]T-NH$_2$	NA	NA
10	Ac-I[CVYQDWGA(NMe)HRC]T-NH$_2$	94	0.03
11	Ac-I[CVYQDWGAH(NMe)RC]T-NH$_2$	32	0.08
12	Ac-I[CVYQDWGAHR(NMe)C]T-NH$_2$	154	0.02
13	Ac-I[CVYQDWGAHRC](NMe)T-NH$_2$	1.9	1.3

[a] Complement inhibition assay based on initiation via the classical pathway.
[b] Relative to peptide **1**. NA: not active at the highest concentrations tested.
[c] Data published previously (Magotti et al., 2009), peptide **1** was used as an internal control.

3. Results

3.1. Inhibition of complement activation

A backbone N-methylation scan was performed on a [Tyr^4]-Ac-compstatin template (peptide **1**) to generate analogues **2**–**13** (Table 1, Suppl. Fig. 1). Although analogue **1** is less potent than the current lead compound, [Trp(Me)^4]-Ac-compstatin, it was chosen for the initial scan because of its lower cost of synthesis (Klepeis et al., 2003; Magotti et al., 2009). The ability of each peptide to inhibit the activation of complement was then evaluated by ELISA and compared to the activity of internal control **1** (Table 1). The most negative effect was observed for the N-methylation of Val^3, Tyr^4 and Ala^9, which rendered analogues **3**, **4**, and **9** completely inactive. In contrast, N-methylation of Gly^8 and Thr^{13} produced analogues **8** and **13** with slightly increased potency (1.7- and 1.3-fold, respectively). N-methylation in all other positions resulted in detectable, yet significantly reduced inhibitory activity (Table 1).

We then applied the findings from the N-methylation scan to the current lead compound, [Trp(Me)^4]-Ac-compstatin (peptide **14**), and synthesized analogues with selective N-methylation and amino acid substitutions at positions 8 and 13 (peptides **15**–**23**; Table 2, Fig. 1). Since previous studies had indicated strict limitations for substituting the side chain at position 8, we restricted our modifications to the absence (Gly^8) or presence of N-methylation (NMeGly^8, i.e. Sar^8) (Furlong et al., 2000; Morikis et al., 1998). In contrast, previous work showed that the C-terminal position 13 allowed more flexibility for substitutions and had even suggested a preference for Ile over Thr (Morikis and Lambris, 2002). We therefore further investigated the importance of position 13 and designed a series of Sar^8 analogues to include various N-methylated, hydrophobic, or aromatic residues in this position (**18**–**23**). Consistent with the results from the N-methylation scan, the introduction of a single N-methyl group at position 8 (Sar^8; peptide **15**) increased the inhibitory potency by 1.3-fold (Table 3). In agreement with previous studies on earlier compstatin analogues (Morikis et al., 2002), replacement of Thr by Ile at position 13 led to a noticeable increase for both the Gly^8 and Sar^8 peptides (analogues **16**, **17**). However, neither the substitution of Ile by Leu (analogue **18**) or Nle (analogue **19**) nor the introduction of His (analogue **22**) or Phe (analogue **23**) produced any improvement over the Ile^{13} analogue **17**. In contrast, N-methylation of both Thr^{13} (analogue **20**) and Ile^{13} (analogue **21**) resulted in a significant increase in inhibitory

Table 2
Evaluation of inhibitory potency, kinetic, and thermodynamic parameters for a series of compstatin analogues (Ac-Ile-[Cys-Val-Trp(Me)-Gln-Asp-Trp-**Xaa**-Ala-His-Arg-Cys]-**Xaa**-NH$_2$) with modifications at positions 8 and 13. k_a: association rate; k_d: dissociation rate; $K_{D,SPR}$: binding constant from SPR; $K_{D,ITC}$: binding constant from ITC; ΔH: enthalpy change; $-T\Delta S$: entropy change; ΔG: free energy change.

No.	Xaa[8]	Xaa[13]	IC$_{50}$ (nM)	k_a (10^6/Ms)	k_d (10^{-3}/s)	$K_{D,SPR}$ (nM)	$K_{D,ITC}$ (nM)	ΔH (kcal/mol)	$-T\Delta S$ (kcal/mol)	ΔG (kcal/mol)
14[a]	Gly	Thr	206	1.0	11.3	11.9	15.0	−17.6	6.9	−10.7
15	Sar	Thr	159	1.3	7.2	5.5	8.5	−11.7	0.6	−11.1
16	Gly	Ile	154	1.0	11.0	11.0	12.1	−16.6	5.7	−10.9
17	Sar	Ile	92	1.5	6.6	4.4	6.3	−14.1	2.9	−11.2
18	Sar	Leu	108	1.3	6.0	4.6	N/D	N/D	N/D	N/D
19	Sar	Nle	109	1.5	6.6	4.4	N/D	N/D	N/D	N/D
20	Sar	(NMe)Thr	86	1.3	5.1	3.9	7.2	−17.5	6.4	−11.1
21	Sar	(NMe)Ile	62	1.5	3.5	2.3	4.5	−17.1	5.7	−11.4
22	Sar	His	160	N/D	N/D	N/D	N/D	N/D	N/D	N/D
23	Sar	Phe	257	N/D	N/D	N/D	N/D	N/D	N/D	N/D

[a] Used as an internal control in all assays, data published previously (Magotti et al., 2009; Katragadda et al., 2006); N/D: not determined.

Fig. 1. Structures of amino acids incorporated in positions 8 and 13, and the most active peptide **21**.

activity (IC$_{50}$ = 86 and 62 nM, respectively), generating the most potent compstatin analogues described thus far (Table 2, 1000-fold improvement compared to the original compstatin (Sahu et al., 2006)).

3.2. Characterization of binding kinetics

Peptides **15–21** were further characterized by SPR in order to evaluate the effect of individual substitutions on the kinetic profile and binding affinity for C3b (Fig. 2; Table 2). In general,

the relative K_D values showed good consistency with the ELISA results (R^2 = 0.79; Table 3; Suppl. Fig. 3). N-methylation of Gly[8] (**14–15**, **16–17**) clearly improved the binding kinetics and affinity, with significant effects on both kinetic rate constants. In contrast, the Thr-to-Ile substitutions (**14–16**, **15–17**) had only slight, yet still beneficial impact on the SPR profiles. Again, the combination of both substitutions (analogue **17**) had a synergistic effect, with a 2.7-fold stronger affinity than peptide **14**, as compared to the impact of the Sar[8] and Ile[13] modifications alone (2.2- and 1.1-fold, respectively). Substitutions at position 13 alone appeared to

Table 3
Relative improvement in the potency and binding parameters of newly designed compstatin analogues when compared to [Trp(Me)^4]-Ac-compstatin (peptide **14**). rP: relative potency change; rk_a: relative change of association rate; rk_d: relative change of dissociation rate; r$K_{D,SPR}$: relative change of binding constant from SPR; r$K_{D,ITC}$: relative change of binding constant from ITC; $\Delta\Delta H$: relative enthalpy change; $-T\Delta\Delta S$: relative entropy change; $\Delta\Delta G$: relative free energy change.

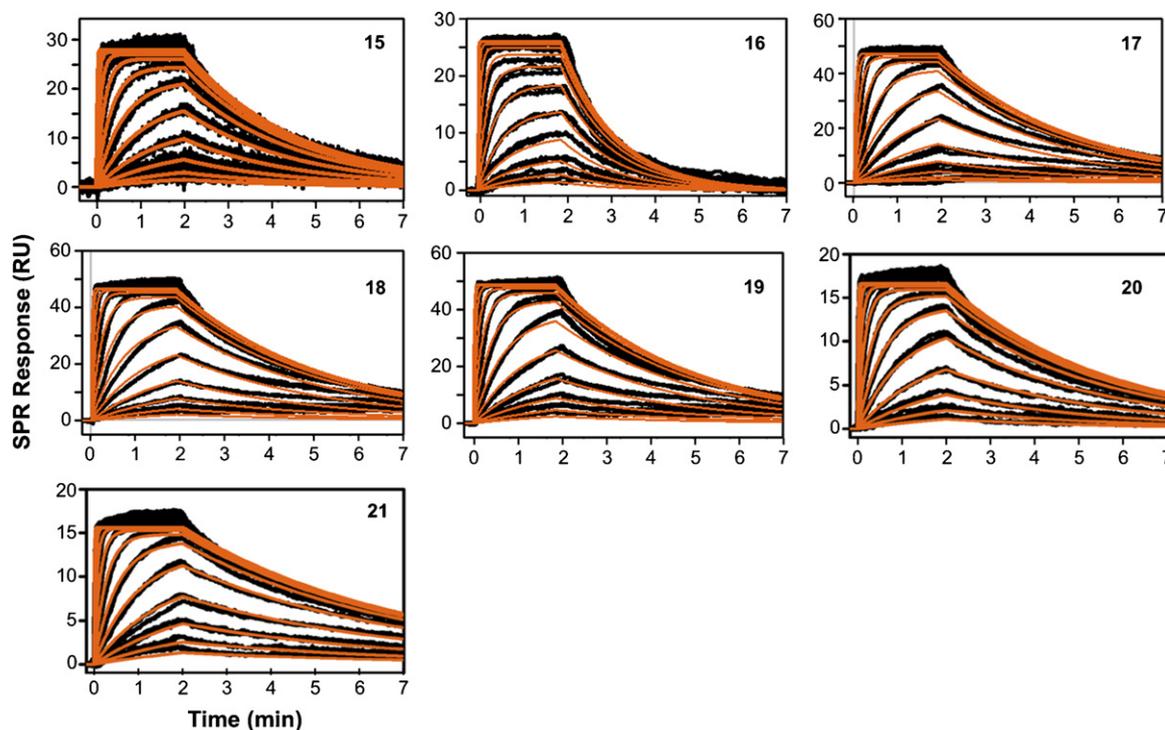| No.	Xaa[8]	Xaa[13]	rP	rk_a	rk_d	r$K_{D,SPR}$	r$K_{D,ITC}$	$\Delta\Delta H$ (kcal/mol)	$-T\Delta\Delta S$ (kcal/mol)	$\Delta\Delta G$ (kcal/mol)
14	Gly	Thr	1.0	1.0	1.0	1.0	1.0	0	0	0
15	Sar	Thr	1.3	1.3	1.6	2.2	1.8	5.9	−6.3	−0.4
16	Gly	Ile	1.3	1.0	1.0	1.1	1.2	1.0	−1.3	−0.2
17	Sar	Ile	2.2	1.5	1.7	2.7	2.4	3.5	−4.1	−0.5
18	Sar	Leu	1.9	1.3	1.9	2.6	N/D	N/D	N/D	N/D
19	Sar	Nle	1.9	1.5	1.7	2.7	N/D	N/D	N/D	N/D
20	Sar	(NMe)Thr	2.4	1.3	2.2	3.1	2.4	0.1	−0.5	−0.4
21	Sar	(NMe)Ile	3.3	1.5	3.2	5.2	3.3	0.5	−1.3	−0.7
22	Sar	His	1.3	N/D	N/D	N/D	N/D	N/D	N/D	N/D
23	Sar	Phe	0.8	N/D	N/D	N/D	N/D	N/D	N/D	N/D

Fig. 2. Characterization of the binding kinetics of the interactions of compstatin analogues with C3b: SPR data representing the binding of peptides **15**–**21** to C3b with processed signals (black) overlaid by the kinetic fit to a 1:1 Langmuir binding isotherm (red). (For interpretation of the references to color in this figure legend, the reader is referred to the web version of the article.)

primarily influence the dissociation rate ($k_d = 3.5–11.0 \times 10^{-3}$ s^{-1}); the association rate remained essentially constant for all Sar^8 analogues ($k_a = 1.3–1.5 \times 10^6$ M^{-1} s^{-1}). In this series, N-methylation of Thr^{13} (analogue **20**) and Ile^{13} (analogue **21**) again had the strongest impact on the dissociation rate, rendering analogue **21** the strongest binder, with a more than 5-fold increase in affinity over peptide **14**. The evaluated isomers of Ile^{13} (Leu, Nle; peptides **18** and **19**) had a negligible influence on the kinetic profile and affinity, indicating a common binding mode for this scaffold.

3.3. Characterization of binding thermodynamics

ITC experiments were performed for peptides **15**–**17** and **20**–**21** in order to correlate the observed effects on affinity and potency with their thermodynamic profiles (Tables 2 and 3; Suppl. Fig. 2). Although the absolute K_D values in ITC tended to be slightly higher than those from SPR, they were very well correlated with the ELISA and SPR results ($R^2 = 0.89$ and 0.96, respectively; Suppl. Fig. 3). The highly beneficial enthalpy value ($\Delta H = -17.6$ kcal/mol) of the
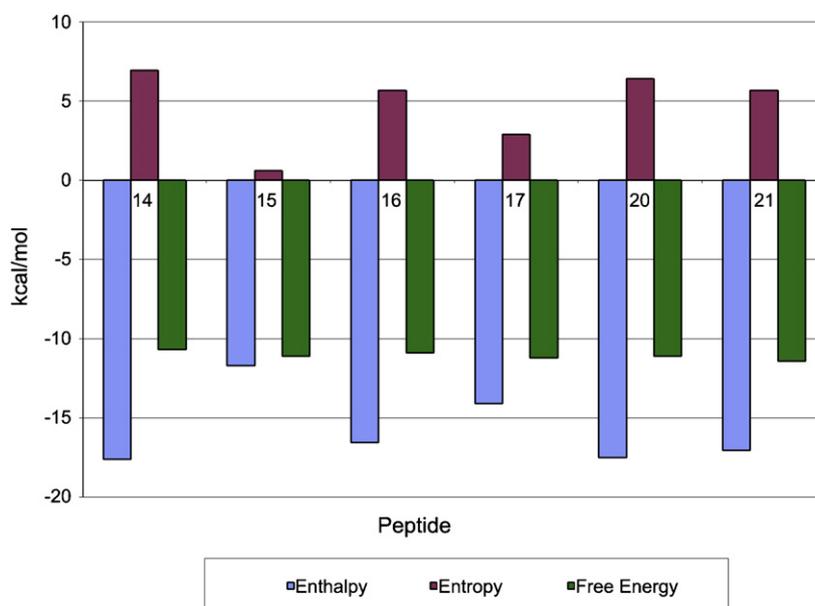
Fig. 3. Comparison of enthalpic and entropic contributions to the binding of peptides **14**–**17** and **20**–**21**.

previous lead compound (peptide **14**) was not surpassed by any of the newly designed analogues. In contrast, the entire panel had significantly improved entropy values ($-T\Delta S = 0.6$–6.4 kcal/mol) when compared to peptide **14** ($-T\Delta S = 6.9$ kcal/mol).

It is interesting to note that peptide **15** (Sar[8]Thr[13]; $-T\Delta S = 0.6$ kcal/mol) exhibited the lowest entropic penalty of all the reported compstatin analogues (Fig. 3). However, the majority of this large entropic gain was offset by a loss of favorable enthalpy ($\Delta\Delta H = 5.9$ kcal/mol). Similar trends were observed for the entire panel (Fig. 2), indicating an enthalpy–entropy compensation effect (Starikov and Norden, 2007). Intriguingly, additional substitution of Ile[13] for Thr[13] as in peptide **17** recaptured some of the lost enthalpy ($\Delta H = -14.1$ kcal/mol), while yielding some of the entropy gain ($-T\Delta S = 2.9$ kcal/mol) in peptide **15**. N-methylation in position 13, as in peptides **20**–**21**, brought their enthalpy values even closer to that of peptide **14**. Overall, the increased binding affinity for these peptides appeared to be mainly achieved by a reduction in entropic penalty. Furthermore, the ITC data confirmed the SPR results and indicated that it was the Sar[8], and not the Ile[13] substitution that contributed most to the largely increased affinity of peptide **17**.

4. Discussion

Using a combination of targeted backbone N-methylation and C-terminal amino acid substitution, we have been able to significantly increase both the binding affinity and inhibitory potency of the clinically important complement inhibitor compstatin. An in-depth biophysical characterization allowed us to dissect the impact of individual modifications on the kinetic and thermodynamic profile of the most active analogues. Since compstatin analogues exert their inhibitory action by binding to the highly abundant plasma protein C3 and its fragments, high target binding affinity and peptide stability are of utmost clinical importance.

Previous optimization attempts have improved the affinities of compstatin analogues from high micromolar to low nanomolar levels, and these improvements in affinity were often accompanied by exceptionally favorable changes in binding enthalpy (Katragadda et al., 2006). However, we also observed that most of the improved compstatin analogues were hampered by similarly large entropic penalties. We envisioned that this effect was the result of both unfavorable conformational changes occurring upon compstatin binding and weak hydrophobic interactions involving compstatin side chains (Lafont et al., 2007).

The common observation that small, flexible ligands can lose a substantial amount of conformational entropy upon binding to a protein is likely to hold true for the rather flexible 11-residue ring of compstatin and its analogues (Chang et al., 2007; Morikis et al., 2002). Previous studies have shown that the bound conformation of [Trp[4]]-Ac-compstatin as observed in the crystal structure is clearly distinct from its free solution conformation obtained from computational and NMR studies (Janssen et al., 2007; Mallik et al., 2005; Mulakala et al., 2007; Tamamis et al., 2007). The large conformational rearrangements required for tight binding to its site in C3 and the accompanying loss of flexibility of the ring structure might therefore both contribute to the entropic penalty (Janssen et al., 2007; Killian et al., 2009). In principle, compstatin analogues with a properly constrained free solution structure that is similar to the bound structure should therefore display a smaller unfavorable binding entropy, and hence an increased binding affinity (Christian et al., 2000; Bohm and Klebe, 1996).

Another possible source of the large unfavorable entropy of compstatin is incomplete desolvation. Desolvation entropy originates from the release of water molecules from both the ligand and its binding pocket during the binding event and is the pre-

dominant force associated with the binding energy of hydrophobic groups (Freire, 2008). Additional hydrophobic moieties and proper orientation of existing hydrophobic side chains in compstatin may therefore allow better hydrophobic contact, and thereby improve desolvation and, consequently, binding affinity.

N-methylation has previously been known to impose local conformational restraints on both the modified residue and its neighbor(s), to affect the solution structure, and to increase the overall lipophilicity of peptides (Biron et al., 2006; Harris et al., 2009; Laufer et al., 2009). We therefore chose this method as the primary optimization approach in our study because of its potential to address both the conformation and desolvation problems at the same time. In addition, N-methylation often increases peptide stability and thereby improves pharmacokinetic properties (Biron et al., 2006). Our initial N-methylation scan revealed several residues with very low tolerance for the modification (e.g., Val[3], Trp[4], and Ala[9]). Most of these residues have previously been identified as sensitive to modifications, and N-methylation may block critical hydrogen bonding, affect side chain orientation toward the binding site or induce unfavorable conformational changes in the peptide (Magotti et al., 2009; Morikis and Lambris, 2002; Ricklin and Lambris, 2008). However, the scan also identified two residues, i.e. Gly[8] and Thr[13], for which N-methylation was beneficial.

4.1. N-methylation of Gly[8] leads to improved hydrophobic interactions

Alterations in the hydrophobic interaction pattern of a peptide usually translate to changes in dissociation rates and entropy values, and can therefore be evaluated by kinetic and thermodynamic methods. Our previous study revealed a striking example of this relationship, in which methylation of the Trp[4] indole nitrogen in [Trp[4]]-Ac-compstatin led to a 13.8-fold increase in affinity that could be attributed to a 13-fold slower k_d and 1.9 kcal/mol less entropic penalty (Magotti et al., 2009). In the current study, both SPR and ITC showed that a single N-methylation of Gly[8] (peptide **15** vs **14**, **17** vs **16**) caused a significant increase in affinity. The large drop in unfavorable entropy, the significantly weaker polar interactions reflected in the high $\Delta\Delta H$, and the slower k_d all suggest contributions from better hydrophobic contacts. Although the co-crystal structure of peptide **14** with C3 or C3b has not yet been determined, its binding mode at position 7 is expected to be similar to [Trp[4]]-Ac-compstatin based on previous SAR studies (Chiu et al., 2008; Janssen et al., 2007; Katragadda et al., 2006; Magotti et al., 2009). Owing to its position and size, the N-methyl group of Sar[8] in peptides **15** and **17** is more likely to improve desolvation indirectly rather than to make direct hydrophobic interactions with C3. It is possible that the presence of the N-methyl group at position 8 could slightly affect (or stabilize) the orientation of the side chain of the vicinal Trp[7] (Laufer et al., 2009). This residue has previously been shown to be sensitive to modification because of its critical role in hydrogen bonding as well as hydrophobic interactions with C3 (Chiu et al., 2008; Janssen et al., 2007; Katragadda et al., 2006; Mallik et al., 2005; Moretto et al., 2006; Morikis et al., 2002).

As a consequence, structural changes induced by N-methylation at position 8 are likely to weaken the hydrogen bonding involving Trp[7] indole nitrogen and allow for a better fit of the Trp[7] indole ring into the hydrophobic binding pocket in C3. Such hydrophobic contacts are usually accompanied by a release of ordered water molecules from the binding site, which is expected to result in improved entropy values. It has been reported that the entropy gain from release of a single water molecule into bulk solvent can be as high as 2.0 kcal/mol (Dunitz, 1994). It is therefore likely that the large change in entropy upon addition of an N-methyl group at posi-

tion 8 between peptides **14** and **15** ($-T\Delta\Delta S = -6.3$ kcal/mol) is at least partially caused by a more efficient release of water molecules. However, additional structural or computational studies are clearly required to further confirm this hypothesis.

4.2. N-methylation of Gly[8] results in stabilization of the bound-like β-turn structure

Analysis of a variety of compstatin analogues including [Trp[4]]-Ac-compstatin using molecular dynamics (MD) simulations and NMR revealed a highly flexible ring structure that features a β-turn comprising residues Gln[5]-Asp[6]-Trp[7]-Gly[8] in solution (Mallik et al., 2003, 2005; Morikis et al., 1998; Tamamis et al., 2007). Although this turn was considered an important structural feature, it was later found that the intrinsic tendency of a compstatin analogue to form a β-turn does not strictly correlate with its inhibitory potency (Morikis et al., 2002; Tamamis et al., 2007). Even more importantly, the C3c-bound structure of [Trp[4]]-Ac-compstatin revealed that the position of the β-turn had shifted considerably from positions 5–8 to 8–11, suggesting a large conformational change that might contribute to the large entropic penalty found for this analogue ($-T\Delta S = 8.8$ kcal/mol) (Janssen et al., 2007; Katragadda et al., 2006). As the requirement for such a conformational adaptation upon binding directly hampers the complex formation efficiency (and thereby the k_a value), induction of a pre-formed 8–11 β-turn in solution is believed to be beneficial.

While detailed solution structures are only available for early compstatin analogues, NOE analysis of a series of more recent analogues, including the potent [2Nal[4]]-Ac-compstatin, still indicated a clear preference to form a 5–8 β-turn despite variations in their side chains (Mallik et al., 2005). As peptide **14** shares positions 5–8 with the 2Nal[4] analogue, it is very likely that this analogue also favors a 5–8 β-turn in solution. Indeed, the k_a rates for both analogues have been found to be very similar in a recent SPR study ($0.8-0.9 \times 10^6$ M^{-1} s^{-1}) (Magotti et al., 2009). In contrast, the SPR results presented in this study revealed a significantly improved k_a for all Sar[8] analogues. It is known that the association rate between two molecules is affected by factors such as long-range electrostatic interactions and conformational adaptations between the binding partners (Schreiber, 2002). Pre-formation of a solution structure that shares a high level of similarity with the bound form will therefore lead to faster ligand recognition and complex formation (as evidenced by a higher k_a). An extreme example of this dependence is the lack of observable activity in the case of linear compstatin analogues, which could be attributed to an extremely slow k_a because of the huge conformational differences between the free and bound forms (Sahu et al., 1996). In the case of Sar[8], analogue **17** showed a 1.5-fold increase in k_a despite a significant loss of hydrogen bonding and other polar interactions ($\Delta\Delta H = 3.5$ kcal/mol). Considering the highly similar electrostatic properties of peptides **14** and **17**, it is very likely that peptide **17** has a larger assembly of favorable conformations than **14** for binding to C3, which may suggest a potential shift from a 5–8 to a 8–11 β-turn by the presence of the N-methyl group. This effect may be accomplished by prohibiting the potential formation of an intramolecular hydrogen bond between residues 5 and 8, and by decreasing the flexibility of the Trp[7]-Gly[8] amide bond, which is consistent with the previously described critical role of Gly[8] for the formation of the 5–8 β-turn (Morikis et al., 1998; Morikis and Lambris, 2002; Wilmot and Thornton, 1988).

In addition to conformational differences in the essential β-turn region, N-methylation at position 8 may also contribute to the reduced entropic penalty by restricting rotations of local backbone bonds and making the free solution structure less flexible. Finally, a general increase in hydrophobicity may also be responsible for the substantial improvement in the dissociation rate for peptide **17**.

Most importantly, the same pattern of improved k_a and k_d values could be observed for all the Sar[8] analogues, thereby directly supporting the finding of a generally beneficial effect of N-methylation at position 8.

4.3. Position 13 is important in potentiating compstatin analogue activity

Thr[13] lies outside the ring structure of compstatin, and initial studies had shown that removal of both flanking residues (Ile[1] and Thr[13]) had comparatively little effect on the inhibitory potency (Morikis et al., 1998). Furthermore, the co-crystal structure of [Trp[4]]-Ac-compstatin later revealed that Thr[13] does not make any contact with the binding site, but rather sticks out into the solvent (Janssen et al., 2007). Despite its allegedly low importance for target recognition, previous substitutions of this residue have indicated that it may nevertheless contribute to peptide activity (Morikis et al., 2002). When we replaced Thr[13] with a diverse panel of amino acids in the present study, we indeed observed distinct effects on the inhibitory potency. In contrast to the rather bulky His[13] and Phe[13], which produced only small or even negative effects, replacement with the smaller but hydrophobic Ile was found to be slightly beneficial. The highly similar effects observed for the two isomers of Ile (i.e., Leu and Nle) suggest that physicochemical and steric properties, rather than specific contacts, may have been responsible for this improvement. However, a more distinct improvement in affinity and activity was observed upon backbone N-methylation of both Thr[13] (analogue **20**) and Ile[13] (analogue **21**). While the observed improvements may have resulted from increased backbone restraints, and hence lower conformational entropic penalties upon binding, it is also possible that the nature of the residue at position 13 can further influence the formation and stabilization of active conformations, either sterically or via formation of intramolecular hydrophobic contacts. However, the high flexibility of this residue makes the elucidation of a detailed mechanism rather difficult. Nevertheless, substitution of Thr[13] not only restored our view about the importance of this flanking position but also resulted in highly potent compstatin analogues.

In conclusion, we have developed a new series of compstatin analogues with significantly improved potency based on N-methylation of the peptide backbone and substitutions at the flanking position 13. The combined assessment of functional, kinetic, and thermodynamic parameters allowed for a dissection of structure–activity relationships. This integrated approach revealed that N-methylation of Gly[8] potentially improves target recognition and complex stability by mechanism that may likely include reinforced bound-like β-turn motifs, increased local backbone constraints and improved hydrophobic interactions involving the side chain of Trp[7]. Although Thr[13] does not form direct contacts with the C3 binding site, replacement of this residue by Ile, with subsequent N-methylation, generated a compstatin analogue with a more than 5-fold improved binding affinity over the previous lead compound. As N-methylation is known to improve peptide plasma stability, the application of this method may even positively affect the pharmacokinetic properties of the optimized compstatin analogues. In fact, the efficacy of peptide **17** has recently been confirmed in an ex vivo hemodialysis model, where it impaired filter-induced activation of complement and neutrophils, as well as reduced the expression of tissue factor that is associated with enhanced risk of thrombosis in dialysis patients (Kourtzelis et al., 2010). The findings of our study therefore not only pave the way for future improvement based on peptide **21**, but also are likely to have a direct impact on the clinical development of promising compstatin analogues for various indications.

Acknowledgments

Appendix A. Supplementary data

Supplementary data associated with this article can be found, in the online version, at doi:10.1016/j.molimm.2010.10.004.

References

Anon., 2009. Deal watch: Alcon licenses complement pathway inhibitor for macular degeneration. Nat. Rev. Drug Discov. 8, 922.

Biron, E., Chatterjee, J., Kessler, H., 2006. Optimized selective N-methylation of peptides on solid support. J. Pept. Sci. 12, 213–219.

Bohm, H.J., Klebe, G., 1996. What can we learn from molecular recognition in protein-ligand complexes for the design of new drugs? Angew. Chem. Int. Ed. 35, 2588–2614.

Carbonell, T., Freire, E., 2005. Binding thermodynamics of statins to HMG-CoA reductase. Biochemistry 44, 11741–11748.

Carroll, M.C., 2008. Complement and humoral immunity. Vaccine 26 (Suppl. 8), I28–I33.

Chang, C.E., Chen, W., Gilson, M.K., 2007. Ligand configurational entropy and protein binding. Proc. Natl. Acad. Sci. U.S.A. 104, 1534–1539.

Chatterjee, J., Gilon, C., Hoffman, A., Kessler, H., 2008. N-methylation of peptides: a new perspective in medicinal chemistry. Acc. Chem. Res. 41, 1331–1342.

Chen, M., Daha, M.R., Kallenberg, C.G., 2010. The complement system in systemic autoimmune disease. J. Autoimmun. 34, J276–J286.

Chiu, T.L., Mulakala, C., Lambris, J.D., Kaznessis, Y.N., 2008. Development of a new pharmacophore model that discriminates active compstatin analogs. Chem. Biol. Drug Des. 72, 249–256.

Christian, E., Schafmeister, J.P., Gregory, L., Verdine, 2000. An all-hydrocarbon cross-linking system for enhancing the helicity and metabolic stability of peptides. J. Am. Chem. Soc. 122, 5891–5892.

Cocchio, C., Marzella, N., 2009. Cinryze, a human plasma-derived C1 esterase inhibitor for prophylaxis of hereditary angioedema. P&T 34, 293–328.

Diepenhorst, G.M., van Gulik, T.M., Hack, C.E., 2009. Complement-mediated ischemia-reperfusion injury: lessons learned from animal and clinical studies. Ann. Surg. 249, 889–899.

Dunitz, J.D., 1994. The entropic cost of bound water in crystals and biomolecules. Science 264, 670.

Fairlie, D.P., Abbenante, G., March, D.R., 1995. Macrocyclic peptidomimetics: forcing peptides into bioactive conformations. Curr. Med. Chem. 2, 654–686.

Freire, E., 2008. Do enthalpy and entropy distinguish first in class from best in class? Drug Discov. Today 13, 869–874.

Furlong, S.T., Dutta, A.S., Coath, M.M., Gormley, J.J., Hubbs, S.J., Lloyd, D., Mauger, R.C., Strimpler, A.M., Sylvester, M.A., Scott, C.W., Edwards, P.D., 2000. C3 activation is inhibited by analogs of compstatin but not by serine protease inhibitors or peptidyl alpha-ketoheterocycles. Immunopharmacology 48, 199–212.

Hammer, C.H., Wirtz, G.H., Renfer, L., Gresham, H.D., Tack, B.F., 1981. Large scale isolation of functionally active components of the human complement system. J. Biol. Chem. 256, 3995–4006.

Harris, K.S., Casey, J.L., Coley, A.M., Karas, J.A., Sabo, J.K., Tan, Y.Y., Dolezal, O., Norton, R.S., Hughes, A.B., Scanlon, D., Foley, M., 2009. Rapid optimization of a peptide inhibitor of malaria parasite invasion by comprehensive N-methyl scanning. J. Biol. Chem. 284, 9361–9371.

Huber, W., 2005. A new strategy for improved secondary screening and lead optimization using high-resolution SPR characterization of compound-target interactions. J. Mol. Recognit. 18, 273–281.

Inoue, N., Murakami, Y., Kinoshita, T., 2003. Molecular genetics of paroxysmal nocturnal hemoglobinuria. Int. J. Hematol. 77, 107–112.

Janssen, B.J., Halff, E.F., Lambris, J.D., Gros, P., 2007. Structure of compstatin in complex with complement component C3c reveals a new mechanism of complement inhibition. J. Biol. Chem. 282, 29241–29247.

Katragadda, M., Magotti, P., Sfyroera, G., Lambris, J.D., 2006. Hydrophobic effect and hydrogen bonds account for the improved activity of a complement inhibitor, compstatin. J. Med. Chem. 49, 4616–4622.

Killian, B.J., Kravitz, J.Y., Somani, S., Dasgupta, P., Pang, Y.P., Gilson, M.K., 2009. Configurational entropy in protein-peptide binding: computational study of Tsg101 ubiquitin E2 variant domain with an HIV-derived PTAP nonapeptide. J. Mol. Biol. 389, 315–335.

Klepeis, J.L., Floudas, C.A., Morikis, D., Tsokos, C.G., Argyropoulos, E., Spruce, L., Lambris, J.D., 2003. Integrated computational and experimental approach for lead optimization and design of compstatin variants with improved activity. J. Am. Chem. Soc. 125, 8422–8423.

Kourtzelis, I., Markiewski, M.M., Doumas, M., Rafail, S., Kambas, K., Mitroulis, I., Panagoutsos, S., Passadakis, P., Vargemezis, V., Magotti, P., Qu, H., Mollnes, T.E., Ritis, K., Lambris, J.D., 2010. Complement anaphylatoxin C5a contributes to hemodialysis-associated thrombosis. Blood 116, 631–639.

Lachmann, P.J., Smith, R.A., 2009. Taking complement to the clinic – has the time finally come? Scand. J. Immunol. 69, 471–478.

Lafont, V., Armstrong, A.A., Ohtaka, H., Kiso, Y., Mario Amzel, L., Freire, E., 2007. Compensating enthalpic and entropic changes hinder binding affinity optimization. Chem. Biol. Drug Des. 69, 413–422.

Laufer, B., Chatterjee, J., Frank, A.O., Kessler, H., 2009. Can N-methylated amino acids serve as substitutes for prolines in conformational design of cyclic pentapeptides? J. Pept. Sci. 15, 141–146.

Magotti, P., Ricklin, D., Qu, H., Wu, Y.Q., Kaznessis, Y.N., Lambris, J.D., 2009. Structure-kinetic relationship analysis of the therapeutic complement inhibitor compstatin. J. Mol. Recognit. 22, 495–505.

Mallik, B., Katragadda, M., Spruce, L.A., Carafides, C., Tsokos, C.G., Morikis, D., Lambris, J.D., 2005. Design and NMR characterization of active analogues of compstatin containing non-natural amino acids. J. Med. Chem. 48, 274–286.

Mallik, B., Lambris, J.D., Morikis, D., 2003. Conformational interconversion in compstatin probed with molecular dynamics simulations. Proteins 53, 130–141.

Markiewski, M.M., DeAngelis, R.A., Benencia, F., Ricklin-Lichtsteiner, S.K., Koutoulaki, A., Gerard, C., Coukos, G., Lambris, J.D., 2008. Modulation of the antitumor immune response by complement. Nat. Immunol. 9, 1225–1235.

Mastellos, D., Morikis, D., Strey, C., Holland, M.C., Lambris, J.D., 2004. From atoms to systems: a cross-disciplinary approach to complement-mediated functions. Mol. Immunol. 41, 153–164.

Mollnes, T.E., Kirschfink, M., 2006. Strategies of therapeutic complement inhibition. Mol. Immunol. 43, 107–121.

Moretto, A., Crisma, M., Kaptein, B., Broxterman, Q.B., Toniolo, C., 2006. N-methylation of N(alpha)-acylated, fully C(alpha)-methylated, linear, folded peptides: synthetic and conformational aspects. Biopolymers 84, 553–565.

Morikis, D., Assa-Munt, N., Sahu, A., Lambris, J.D., 1998. Solution structure of compstatin, a potent complement inhibitor. Protein Sci. 7, 619–627.

Morikis, D., Lambris, J.D., 2002. Structural aspects and design of low-molecular-mass complement inhibitors. Biochem. Soc. Trans. 30, 1026–1036.

Morikis, D., Roy, M., Sahu, A., Troganis, A., Jennings, P.A., Tsokos, G.C., Lambris, J.D., 2002. The structural basis of compstatin activity examined by structure-function-based design of peptide analogs and NMR. J. Biol. Chem. 277, 14942–14953.

Mulakala, C., Lambris, J.D., Kaznessis, Y., 2007. A simple, yet highly accurate, QSAR model captures the complement inhibitory activity of compstatin. Bioorg. Med. Chem. 15, 1638–1644.

Qu, H., Magotti, P., Ricklin, D., Lambris, J.D., 2009a. Development of compstatin derivative-albumin binding peptide chimeras for prolonged plasma half-life. In: Lebl, M. (Ed.), The 21st American Peptide Symposium. Bloomington, IN, U.S.A, pp. 219–220.

Qu, H., Ricklin, D., Lambris, J.D., 2009b. Recent developments in low molecular weight complement inhibitors. Mol. Immunol. 47, 185–195.

Ricklin, D., Hajishengallis, G., Yang, K., Lambris, J.D., 2010. Complement: a key system for immune surveillance and homeostasis. Nat. Immunol. 11, 785–797.

Ricklin, D., Lambris, J.D., 2007. Complement-targeted therapeutics. Nat. Biotechnol. 25, 1265–1275.

Ricklin, D., Lambris, J.D., 2008. Compstatin: a complement inhibitor on its way to clinical application. Adv. Exp. Med. Biol. 632, 273–292.

Rother, R.P., Rollins, S.A., Mojcik, C.F., Brodsky, R.A., Bell, L., 2007. Discovery and development of the complement inhibitor eculizumab for the treatment of paroxysmal nocturnal hemoglobinuria. Nat. Biotechnol. 25, 1256–1264.

Rovero, P., Pestellini, V., Patacchini, R., Santicioli, P., Maggi, C.A., Meli, A., 1989. Conformationally constrained tachykinins: N-methylated analogues of neurokinin A. Biopolymers 28, 65–67.

Sahu, A., Kay, B.K., Lambris, J.D., 1996. Inhibition of human complement by a C3-binding peptide isolated from a phage-displayed random peptide library. J. Immunol. 157, 884–891.

Sahu, A., Soulika, A.M., Morikis, D., Spruce, L., Moore, W.T., Lambris, J.D., 2000. Binding kinetics, structure-activity relationship, and biotransformation of the complement inhibitor compstatin. J. Immunol. 165, 2491–2499.

Sarver, R.W., Peevers, J., Cody, W.L., Ciske, F.L., Dyer, J., Emerson, S.D., Hagadorn, J.C., Holsworth, D.D., Jalaie, M., Kaufman, M., Mastronardi, M., McConnell, P., Powell, N.A., Quin 3rd, J., Van Huis, C.A., Zhang, E., Mochalkin, I., 2007. Binding thermodynamics of substituted diaminopyrimidine renin inhibitors. Anal. Biochem. 360, 30–40.

Schreiber, G., 2002. Kinetic studies of protein-protein interactions. Curr. Opin. Struct. Biol. 12, 41–47.

Silasi-Mansat, R., Zhu, H., Popescu, N.I., Peer, G., Sfyroera, G., Magotti, P., Ivanciu, L., Lupu, C., Mollnes, T.E., Taylor, F.B., Kinasewitz, G., Lambris, J.D., Lupu, F., 2010. Complement inhibition decreases the procoagulant response and confers organ protection in a baboon model of Escherichia coli sepsis. Blood 116, 1002–1010.

Sjoberg, A.P., Trouw, L.A., Blom, A.M., 2009. Complement activation and inhibition: a delicate balance. Trends Immunol. 30, 83–90.

Soulika, A.M., Khan, M.M., Hattori, T., Bowen, F.W., Richardson, B.A., Hack, C.E., Sahu, A., Edmunds Jr., L.H., Lambris, J.D., 2000. Inhibition of heparin/protamine complex-induced complement activation by compstatin in baboons. Clin. Immunol. 96, 212–221.

Soulika, A.M., Morikis, D., Sarrias, M.R., Roy, M., Spruce, L.A., Sahu, A., Lambris, J.D., 2003. Studies of structure-activity relations of complement inhibitor compstatin. J. Immunol. 171, 1881–1890.

Starikov, E.B., Norden, B., 2007. Enthalpy–entropy compensation: a phantom or something useful? J. Phys. Chem. B 111, 14431–14435.

Tamamis, P., Skourtis, S.S., Morikis, D., Lambris, J.D., Archontis, G., 2007. Conformational analysis of compstatin analogues with molecular dynamics simulations in explicit water. J. Mol. Graph. Model. 26, 571–580.

Weisman, H.F., Bartow, T., Leppo, M.K., Marsh Jr., H.C., Carson, G.R., Concino, M.F., Boyle, M.P., Roux, K.H., Weisfeldt, M.L., Fearon, D.T., 1990. Soluble human complement receptor type 1: in vivo inhibitor of complement suppressing post-ischemic myocardial inflammation and necrosis. Science 249, 146–151.

Weltrowska, G., Berezowska, I., Lemieux, C., Chung, N.N., Wilkes, B.C., Schiller, P.W., 2010. N-methylated cyclic enkephalin analogues retain high opioid receptor binding affinity. Chem. Biol. Drug Des. 75, 182–188.

Wilmot, C.M., Thornton, J.M., 1988. Analysis and prediction of the different types of beta-turn in proteins. J. Mol. Biol. 203, 221–232.

Zhu, J., Chen, T., Chen, L., Lu, W., Che, P., Huang, J., Li, H., Li, J., Jiang, H., 2009. 2-Amido-3-(1H-indol-3-yl)-N-substituted-propanamides as a new class of falcipain-2 inhibitors. 1. Design, synthesis, biological evaluation and binding model studies. Molecules 14, 494–508.